Original Article

Comparison of dimensions and functional features of mitral and tricuspid annuli in the same healthy adults: insights from the three-dimensional speckle-tracking echocardiographic MAGYAR-Healthy Study

Attila Nemes, Árpád Kormányos, Csaba Lengyel

Department of Medicine, Albert Szent-Györgyi Medical School, University of Szeged, Szeged, Hungary

Contributions: (I) Conception and design: A Nemes; (II) Administrative support: Á Kormányos; (III) Provision of study materials or patients: A Nemes, Á Kormányos; (IV) Collection and assembly of data: Á Kormányos; (V) Data analysis and interpretation: Á Kormányos; (VI) Manuscript writing: All authors; (VII) Final approval of manuscript: All authors.

Correspondence to: Attila Nemes, MD, PhD, DSc. Department of Medicine, Albert Szent-Györgyi Medical School, University of Szeged, Semmelweis Street 8, P.O. Box 427, H-6725 Szeged, Hungary. Email: nemes.attila@med.u-szeged.hu.

Background: Evaluation of mitral (MA) and tricuspid annuli (TA) in the same healthy subject in a non-invasive way in real-life clinical settings makes an opportunity to compare their dimensions and derived functional properties. The purpose of the present cohort study was to investigate whether there are any differences in the three-dimensional speckle-tracking echocardiography- (3DSTE-) measured size and derived functional characteristics of the MA and TA in the same healthy adults.

Methods: The study comprised 248 healthy adults, in which 3DSTE was performed to determine MA and TA dimensions and functional properties. Due to insufficient image quality, 89 cases were excluded, therefore the remaining population consisted of 159 subjects (age: 35.6±12.9 years, 76 males). Subjects were enrolled on a voluntary basis consecutively between January 2011 and November 2017 in the outpatient clinic of the tertiary cardiology center at the Department of Medicine, University of Szeged, Hungary. Data were analyzed by Student's *t*-test, analysis of variance (ANOVA) test, Fischer's exact test, Pearsons' correlations, interclass correlations and Bland-Altman tests.

Results: Same-side MA/TA end-diastolic annular dilation is associated with simultaneous MA/TA end-systolic dilation and vice versa. MA dilation in end-diastole and end-systole results in MA functional improvement/deterioration. Dilation of end-diastolic TA dimensions does not obviously entail differences in TA function. However, similar to MA, more dilated TA in end-systole is associated with impaired TA function. Dilated MA dimensions (end-diastolic MA area: 4.31±0.62 *vs.* 10.89±1.18 cm^2, P<0.05) are not obviously associated with dilated end-diastolic TA dimensions (area: 7.05±1.42 *vs.* 7.81±1.48 cm^2, P=ns) and functional improvement/impairment (fractional area change: 27.5%±10.8% *vs.* 25.2%±10.6%, P=ns).

Conclusions: Dilation of MA and TA is associated with different contralateral responses in morphology and function.

Keywords: Three-dimensional (3D); echocardiography; mitral; tricuspid; annulus

Submitted Mar 27, 2024. Accepted for publication Jul 22, 2024. Published online Aug 22, 2024.
doi: 10.21037/qims-24-630
View this article at: https://dx.doi.org/10.21037/qims-24-630

Introduction

The accurate determination of valvular dimensions is of clinical importance due to increased possibilities of care for valvular pathologies (1-6). Theoretically, the ideal method is characterized by its non-invasivity, simplicity, ease of implementation and easy-to-learn/easy-to-perform nature. These conditions are met by three-dimensional speckle-tracking echocardiography (3DSTE), which is capable not only for heart chamber quantifications, but also for determination of dimensions and functional properties of annuli of the atrioventricular valves with well-defined normal reference values (7-12). Evaluation of mitral (MA) and tricuspid annuli (TA) in the same healthy subject in a non-invasive way in real-life clinical settings makes an opportunity to compare their dimensions and derived functional properties. Annuli of the atrioventricular valves have a known relationship with left/right ventricles (LV/RV) and atria (LA/RA) (13-16). Due to differences in shape and function of these cardiac chambers and mitral/tricuspid valvular structure and leaflet numbers, it is reasonable to assume that there might be differences between MA and TA dimensions (13,16,17). Moreover, it would be important to know how the morphological and functional features of the MA/TA look and behave even in the presence of smaller/larger than average sized valves. Therefore, the present cohort study aimed to investigate whether there are differences in the size and functional characteristics of the MA/TA as assessed by 3DSTE in the same healthy adults. We present this article in accordance with the STROBE reporting checklist (available at https://qims.amegroups.com/article/view/10.21037/qims-24-630/rc).

Methods

Subject population

The study comprised 248 healthy adults, in which 3DSTE was performed to determine MA and TA dimensions and functional properties. Due to insufficient image quality, 89 cases were excluded, therefore the remaining population consisted of 159 subjects (age: 35.6±12.9 years, 76 males) (*Figure 1*). All of them participated in the tests on a voluntary basis between January 2011 and November 2017 in the outpatient clinic of the tertiary cardiology center at the Department of Medicine, University of Szeged, Hungary. In all healthy individuals, physical examination, laboratory test, standard 12-lead electrocardiography (ECG), and two-dimensional (2D) Doppler echocardiography were performed with findings being in the normal range. None of the participants took any medications regularly, was obese (body mass index >30 kg/m^2) or smoker. All subjects were without any positive medical history including known disorder, previous operation or other pathological state. 3DSTE was also performed in all healthy volunteers: as a first step digital 3D echocardiographic data acquisition was performed at the same time, when 2D echocardiography was performed. As a second step, valve specific analysis was completed at a later date offline. The present study serves as a part of the 'Motion Analysis of the heart and Great vessels bY three-dimensionAl speckle-tRacking echocardiography in Healthy subjects' (MAGYAR-Healthy Study), which has been conducted at the University of Szeged (11,12). Among other purposes, the aim of the present study was to perform analyses that can be used to clarify physiological relationships between parameters measurable during 3DSTE ('Magyar' means 'Hungarian' in Hungarian language). The present study was conducted in accordance with the Declaration of Helsinki (as revised in 2013) and the Institutional and Regional Human Biomedical Research Committee of University of Szeged, Hungary (No. 71/2011) approved the study. All study participants gave written informed consent.

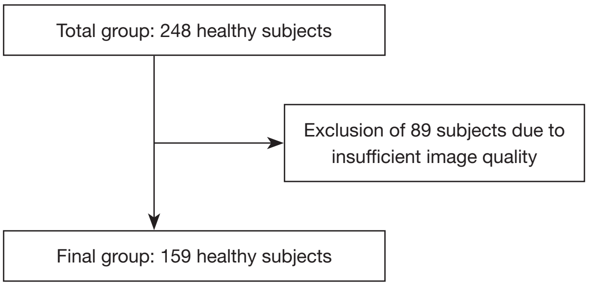

Figure 1 Inclusion and exclusion criteria for healthy subjects involved in the study are presented.

2D Doppler echocardiography

Routine 2D echocardiographic examination was performed in all cases including chamber quantifications with measurement of LA and LV dimensions and LV ejection fraction (EF) by modified Simpsons' method. A Toshiba Artida® echocardiographic machine (Toshiba Medical Systems, Tokyo, Japan) attached to a 1–5 MHz broadband PST-30BT phased-array transducer was used for all examinations. Doppler echocardiography was used for

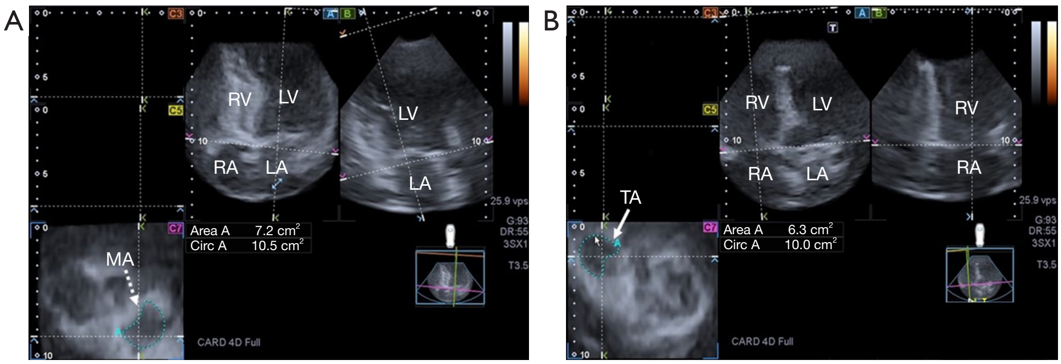

Figure 2 3D echocardiographic assessment of mitral (A) and tricuspid (B) annuli: (A) apical four-chamber view, (B) apical two-chamber view and cross-sectional view (C7) of the mitral and tricuspid annuli optimalised on (A) and (B) images. Mitral and tricuspid annular planes are indicated by dashed white arrow and white arrow, respectively. RV, right ventricle; LV, left ventricle; RA, right atrium; LA, left atrium; Area, mitral/tricuspid annular area; Circ, mitral/tricuspid annular perimeter; MA, mitral annulus; TA, tricuspid annulus; 3D, three-dimensional.

determination of valvular regurgitations and stenoses and to measure early (E) and late (A) diastolic velocities of transmitral flow and their ratio (E/A) (17).

3DSTE

The same Toshiba Artida™ cardiac ultrasound tool (Toshiba Medical Systems, Tokyo, Japan) was used for 3D data acquisitions with a PST-25SX matrix-array transducer with 3D capability (7-12). Data acquisitions were performed from the apical window, when 6 subvolumes were acquired within 6 cardiac cycles. Subjects were asked to hold their breath during that time. For offline data analysis at a later date, vendor-derived software named 3D Wall Motion Tracking (Toshiba Medical Systems, Tokyo, Japan, version 2.7) was used.

3DSTE-derived MA/TA measurements

ECG was used to determine end-systole (at the end of T wave) and end-diastole (at the time of peak R wave). MA and TA were determined on optimized image planes, which were defined on the septal and lateral endpoints of the MA/TA on apical two- and four-chamber views. On C7 short-axis view, the following MA/TA dimensions were calculated at end-diastole (D) and at end-systole (S) (*Figure 2*):

- ❖ MA/TA dimensions (11,12):
  - MA/TA diameter (MAD/TAD): perpendicular line connecting the peak of MA/TA curvature and the middle of the straight MA/TA border;
  - MA/TA area (MAA/TAA) measured by planimetry,
  - MA/TA perimeter (MAP/TAP) measured by planimetry.
- ❖ MA/TA functional properties (11,12):
  - MA/TA fractional shortening (MAFS/TAFS) = (end-diastolic MAD/TAD − end-systolic MAD/TAD)/end-diastolic MAD/TAD × 100;
  - MA/TA fractional area change (MAFAC/TAFAC) = (end-diastolic MAA/TAA − end-systolic MAA/TAA)/end-diastolic MAA/TAA × 100.

Statistical analysis

Continuous and categorical data were expressed in mean ± standard deviation (SD) format or counts and percentages (%) format, as appropriate. $P<0.05$ was considered to be statistically significant. Fischer's exact test was used for all categorical variables. Student's *t*-test with Welch correction and one-way analysis of variance (ANOVA) test with Bonferroni correction were used, where appropriate. For correlations, Pearson's correlation coefficients were determined. The Bland-Altman method was used to determine intraobserver and interobserver agreements. For intraobserver and interobserver correlations, intraclass correlation coefficients (ICCs) were calculated. MedCalc software (MedCalc, Inc., Mariakerke, Belgium) was used for statistical analyses.

Results

Clinical, 2D Doppler echocardiographic data

Clinical and 2D Doppler echo data are presented in *Table 1*.

Table 1 Clinical and two-dimensional echocardiographic data

Data	Measures
Clinical data	
n	159
Mean age (years)	35.6±12.9
Males	76 (48)
Systolic blood pressure (mmHg)	118±5
Diastolic blood pressure (mmHg)	77±6
Heart rate (1/s)	73±2
Weight (kg)	73.3±18.1
Height (cm)	171.7±11.4
Two-dimensional echocardiographic data	
LA diameter (mm)	37.5±3.6
LV end-diastolic diameter (mm)	48.3±3.7
LV end-systolic diameter (mm)	32.4±3.5
LV end-diastolic volume (mL)	107.9±27.0
LV end-systolic volume (mL)	38.3±10.0
Interventricular septum (mm)	9.2±1.2
LV posterior wall (mm)	9.3±1.4
LV ejection fraction (%)	64.7±3.8
Early diastolic mitral inflow velocity - E (cm/s)	79.8±15.8
Late diastolic mitral inflow velocity - A (cm/s)	59.8±14.4

Data are presented as number (percent) or mean ± standard deviation. LA, left atrial; LV, left ventricular.

Cases with larger than grade 1 (functional) mitral (FMR), tricuspid (FTR), aortic or pulmonary functional regurgitations were excluded from the study. None of the subjects showed early signs of valvular stenosis on any valves.

Classification of subjects

Mean ± SD of 3DSTE-derived MA and TA parameters of healthy subjects are presented in *Table 2*. Healthy subjects were classified into 3 groups according to the normal MAD-D, MAA-D, MAP-D, MAD-S, MAA-S, MAP-S, TAD-D, TAA-D, TAP-D, TAD-S, TAA-S and TAP-S: estimated mean ± SD served as the lower (2.00 cm, 5.14 cm^2, 8.75 cm, 1.24 cm, 2.28 cm^2, 5.96 cm, 2.02 cm, 5.73 cm^2, 9.32 cm, 1.56 cm, 3.93 cm^2 and 7.94 cm, respectively) and upper (2.86 cm, 9.44 cm^2, 11.69 cm, 2 cm, 4.74 cm^2, 8.32 cm, 2.66 cm, 9.03 cm^2, 11.66 cm, 2.14 cm, 6.93 cm^2 and 10.2 cm, respectively) values (*Table 2*).

Table 2 Three-dimensional speckle-tracking echocardiography-derived mitral and tricuspid annular dimensions and functional properties

Parameters	Measures (mean ± SD)
MAD-D (cm)	2.43±0.43*
MAA-D (cm^2)	7.29±2.15
MAP-D (cm)	10.22±1.47
MAD-S (cm)	1.62±0.38*
MAA-S (cm^2)	3.51±1.23*
MAP-S (cm)	7.14±1.18*
MAFAC (%)	50.1±15.6*
MAFS (%)	32.3±15.1*
TAD-D (cm)	2.34±0.32
TAA-D (cm^2)	7.38±1.65
TAP-D (cm)	10.49±1.17
TAD-S (cm)	1.85±0.29
TAA-S (cm^2)	5.43±1.50
TAP-S (cm)	9.07±1.13
TAFAC (%)	26.80±11.98
TAFS (%)	20.52± 8.77

*, $P<0.05$ *vs.* TA counterpart. SD, standard deviation; MAD, mitral annular diameter; MAA, mitral annular area; MAP, mitral annular perimeter; MAFAC, mitral annular fractional area change; MAFS, mitral annular fractional shortening; TAD, tricuspid annular diameter; TAA, tricuspid annular area; TAP, tricuspid annular perimeter; TAFAC, tricuspid annular fractional area change; TAFS, tricuspid annular fractional shortening; D, end-diastolic; S, end-systolic; TA, tricuspid annular.

End-diastolic MA dimensions and TA

Almost all MA dimensions were smaller and functional properties were higher as compared to their TA counterpart. Bigger end-diastolic MA dimensions were associated with simultaneous enlargement of end-systolic MA dimensions and larger MA functional properties. However, most TA dimensions showed only tendentious dilation with preserved TA function (*Table 3*).

End-systolic MA dimensions and TA

Almost all MA dimensions were smaller and functional

Table 3 Mitral and tricuspid annular parameters in different end-diastolic mitral annular groups

Parameters	MAD-D ≤2 cm (n=30)	2 cm < MAD-D <2.86 cm (n=104)	2.86 cm ≤ MAD-D (n=25)	MAA-D ≤5.14 cm^2 (n=27)	5.14 cm^2 < MAA-D <9.44 cm^2 (n=107)	9.44 cm^2 ≤ MAA-D (n=25)	MAP-D ≤8.75 cm (n=25)	8.75 cm < MAP-D <11.69 cm (n=106)	11.69 cm ≤ MAP-D (n=28)
MAD-S (cm)	1.40±0.23*	1.65±0.40*†	1.77±0.32†	1.41±0.23*	1.63±0.39*†	1.83±0.38†‡	1.45±0.23*	1.62±0.39*†	1.79±0.40†‡
MAA-S (cm^2)	2.74±0.72*	3.56±1.22*†	4.25±1.26*†‡	2.61±0.64*	3.50±1.16*†	4.50±1.25*†‡	2.66±0.63*	3.49±1.15*†	4.43±1.37*†‡
MAP-S (cm)	6.50±1.01*	7.14±1.13*†	7.96±1.09*†‡	6.22±0.88*	7.14±1.08*†	8.12±1.09*†‡	6.23±0.81*	7.13±1.08*†	7.99±1.20*†‡
MAD-D (cm)	1.87±0.15*	2.43±0.22*†	3.14±0.24*†‡	1.96±0.25*	2.44±0.34*†	2.92±0.34*†‡	2.00±0.23*	2.42±0.37†	2.86±0.34*†‡
MAA-D (mm^2)	4.86±1.10*	7.34±1.56†	10.10±1.78*†‡	4.31±0.62*	7.20±1.07†	10.89±1.18*†‡	4.35±0.70*	7.10±1.16†	10.61±1.35*†‡
MAP-D (cm)	8.66±1.15*	10.31±1.16†	11.78±1.12*†‡	8.07±0.69*	10.24±0.79*†	12.45±0.75*†‡	7.95±0.57*	10.17±0.73*†	12.44±0.70*†‡
MAFAC (%)	40.0±15.8*	50.7±15.6*†	57.6±10.4*†‡	38.9±14.5*	50.9±15.4*†	58.7±10.0*†‡	38.4±13.7*	50.4±15.2*†	59.3±11.8*†‡
MAFS (%)	24.7±11.4	32.0±15.4*†	43.6±10.4*†‡	27.5±11.5*	32.5±15.6*	36.7±14.8*†	27.1±11.4*	32.4±15.6*	37.0±14.6*
TAD-S (cm)	1.76±0.22	1.89±0.32†	1.81±0.22	1.84±0.25	1.84±0.32	1.89±0.21	1.81±0.25	1.86±0.32	1.86±0.21
TAA-S (cm^2)	5.00±1.03	5.55±1.62	5.47±1.34	5.11±1.30	5.42±1.53	5.85±1.47	4.97±1.41	5.47±1.50	5.71±1.47
TAP-S (cm)	8.76±0.88	9.12±1.20	9.24±0.96	8.84±1.15	9.04±1.11	9.44±1.05†	8.67±1.27	9.09±1.08	9.36±1.04†
TAD-D (cm)	2.23±0.30	2.35±0.33	2.43±0.24†	2.30±0.34	2.33±0.32	2.44±0.28	2.26±0.35	2.34±0.31	2.42±0.30
TAA-D (cm^2)	6.97±1.23	7.45±1.78	7.62±1.43	7.05±1.42	7.36±1.72	7.81±1.48	6.88±1.42	7.38±1.69	7.83±1.54†
TAP-D (cm)	10.34±1.02	10.52±1.23	10.56±1.06	10.21±1.10	10.51±1.20	10.73±1.06	10.12±1.08	10.50±1.18	10.77±1.12†
TAFAC (%)	28.0±10.3	26.1±12.8	28.2±10.2	27.5±10.8	27.0±12.6	25.2±10.6	28.2±11.3	26.4±12.4	26.9±10.9
TAFS (%)	20.3±8.2	19.5±8.3	25.1±9.8†‡	19.4±7.8	20.4±9.2	22.0±7.8	19.4±8.0	20.3±9.0	22.4±8.3

Data are presented as mean ± standard deviation. *, P<0.05 *vs.* TA counterpart; †, P<0.05 *vs.* matching mean – SD MA end-diastolic dimension; ‡, P<0.05 *vs.* matching mean MA end-diastolic dimension. MAD, mitral annular diameter; D, end-diastolic; MAA, mitral annular area; MAP, mitral annular perimeter; S, end-systolic; MAFAC, mitral annular fractional area change; MAFS, mitral annular fractional shortening; TAD, tricuspid annular diameter; TAA, tricuspid annular area; TAP, tricuspid annular perimeter; TAFAC, tricuspid annular fractional area change; TAFS, tricuspid annular fractional shortening; TA, tricuspid annular; SD, standard deviation; MA, mitral annulus.

properties were higher as compared to their TA counterpart. Bigger end-systolic dimensions of the MA were associated with simultaneous enlargement of end-diastolic dimensions of the MA and lower MA functional properties. However, most end-diastolic and end-systolic TA dimensions showed only tendentious dilation with preserved TA function (*Table 4*).

End-diastolic TA dimensions and MA

Almost all TA dimensions were larger and functional properties were lower as compared to their MA counterpart. Dilation of end-diastolic TA dimensions was associated with simultaneous dilation of end-systolic TA dimensions and preservation/reduction of most TA functional properties. When TA end-diastolic diameter was the biggest, end-systolic MA dimensions showed simultaneous enlargement. When end-diastolic TA area and perimeter were examined, end-systolic MA dimensions showed only tendentious differences. End-diastolic MA dimensions were tendentiously dilated with dilation of end-diastolic TA dimensions. MA functional properties deteriorated with bigger end-diastolic TA diameter and remained preserved with bigger end-diastolic TA area. With the biggest end-diastolic TA perimeter, the largest MAFAC could be detected (*Table 5*).

End-systolic TA dimensions and MA

Almost all TA dimensions were larger and functional properties were lower as compared to their MA counterpart. Bigger end-systolic TA dimensions were associated with

Table 4 Mitral and tricuspid annular parameters in different end-systolic mitral annular groups

Parameters	MAD-S ≤1.24 cm (n=27)	1.24 cm < MAD-S <2 cm (n=101)	2 cm ≤ MAD-S (n=31)	MAA-S ≤2.28 cm^2 (n=28)	2.28 cm^2 < MAA-S <4.74 cm^2 (n=108)	4.74 cm^2 ≤ MAA-S (n=23)	MAP-S ≤5.96 cm (n=28)	5.96 cm < MAP-S <8.32 cm (n=111)	8.32 cm ≤ MAP-S (n=20)
MAD-S (cm)	1.12±0.14*	1.58±0.19*†	2.22±0.18*†‡	1.22±0.12*	1.61±0.31*†	2.15±0.27*†‡	1.23±0.14*	1.64±0.33*†	2.09±0.36†‡
MAA-S (cm^2)	2.26±0.59*	3.34±0.83*†	5.15±1.03†‡	1.95±0.19*	3.43±0.66*†	5.70±0.79†‡	2.01±0.24*	3.49±0.74*†	5.69±0.95†‡
MAP-S (cm)	6.05±0.94*	7.03±0.90*†	8.45±0.96*†‡	5.49±0.34*	7.16±0.68*†	9.00±0.75†‡	5.51±0.31*	7.18±0.67*†	9.16±0.70†‡
MAD-D (cm)	2.19±0.34	2.42±0.44†	2.71±0.30*†‡	2.18±0.32	2.43±0.42†	2.77±0.35*†‡	2.18±0.32	2.45±0.41*†	2.69±0.45†‡
MAA-D (cm^2)	6.34±1.78	7.05±2.06	8.88±1.91*†‡	6.05±1.79*	7.16±2.01†	9.34±1.74*†‡	6.09±1.74*	7.32±2.04†	8.90±2.17†‡
MAP-D (cm)	9.61±1.37*	10.08±1.40*	11.21±1.29*†‡	9.43±1.41*	10.13±1.37*†	11.55±1.07*†‡	9.45±1.38*	10.22±1.40†	11.37±1.20†‡
MAFAC (%)	61.2±15.5*	50.1±14.2*†	40.3±13.5*†‡	64.7±11.7*	49.1±14.1*†	37.3±12.8*†‡	64.0±12.0*	49.7±13.7*†	33.6±13.3*†‡
MAFS (%)	47.4±10.7*	33.1±12.5*†	16.9±11.1*†‡	42.7±10.4*	32.2±14.6*†	20.9±13.7†‡	42.1±10.9*	31.9±14.8*†	21.3±14.2†‡
TAD-S (cm)	1.78±0.27	1.85±0.29	1.91±0.30	1.81±0.27	1.84±0.30	1.96±0.25†	1.80±0.18	1.85±0.32	1.94±0.27†
TAA-S (cm^2)	5.04±1.27	5.50±1.51	5.57±1.57	5.30±1.43	5.35±1.50	5.96±1.44	5.26±1.30	5.34±1.52	6.18±1.40†‡
TAP-S (cm)	8.79±1.04	9.12±1.15	9.13±1.08	9.10±1.13	8.98±1.14	9.43±0.98	9.04±1.14	8.99±1.14	9.59±0.88‡
TAD-D (cm)	2.20±0.29	2.34±0.33	2.45±0.25†	2.22±0.29	2.33±0.32	2.50±0.26†‡	2.21±0.26	2.35±0.33†	2.49±0.23†
TAA-D (cm^2)	6.82±1.59	7.43±1.64	7.72±1.61†	7.12±1.69	7.31±1.64	8.03±1.6†‡	7.08±1.48	7.36±1.70	8.09±1.34†
TAP-D (cm)	10.21±1.20	10.55±1.15	10.55±1.17	10.50±1.26	10.42±1.16	10.81±1.03	10.52±1.20	10.43±1.19	10.87±0.90
TAFAC (%)	26.0±9.3	26.8±12.8	28.1±10.9	25.6±10.1	27.5±12.6	25.8±10.3	25.6±9.8	28.2±12.5	23.6±9.9
TAFS (%)	18.8±8.4	20.7±8.8	22.2±8.7	18.3±9.2	21.0±8.8	21.6±7.5	18.0±8.3	21.2±8.7	21.7±9.8

Data are presented as mean ± standard deviation. *, P<0.05 *vs.* TA counterpart; †, P<0.05 *vs.* matching mean – SD MA end-systolic dimension; ‡, P<0.05 *vs.* matching mean MA end-systolic dimension. MAD, mitral annular diameter; S, end-systolic; MAA, mitral annular area; MAP, mitral annular perimeter; D, end-diastolic; MAFAC, mitral annular fractional area change; MAFS, mitral annular fractional shortening; TAD, tricuspid annular diameter; TAA, tricuspid annular area; TAP, tricuspid annular perimeter; TAFAC, tricuspid annular fractional area change; TAFS, tricuspid annular fractional shortening; TA, tricuspid annular; SD, standard deviation; MA, mitral annulus.

simultaneous enlargement of end-diastolic TA dimensions, reduction of TA functional properties and (tendentious) dilation of end-diastolic and end-systolic MA dimensions with (mostly) preserved MA function (*Table 6*).

Reproducibility of 3D echocardiography-derived MA/TA measurements

3DSTE-derived end-diastolic and end-systolic MA/TA diameter, area, and perimeter measured two times by the same observer (intraobserver agreement) and by two independent observers (interobserver agreement) were expressed as mean ± 2SD together with ICCs, the results are demonstrated in *Table 7*. Assessments were performed on 30 randomly selected subjects.

Feasibility of 3D echocardiography-derived MA/TA measurements

Images of 89 out of 248 healthy subjects (36%) were inadequate for visual MA or TA qualitative analysis with or without artifacts therefore had to be excluded. The overall feasibility of MA/TA measurements proved to be 64%.

Discussion

Although there are many similarities between the atrioventricular valves and their annuli, they are fundamentally different (13-16). Both mitral and tricuspid valves have a spatial saddle-shape with a fibrous structure and these valves are attached to the ventricular walls with tendineal chords and papillary muscles, the number of leaflets differ.

Table 5 Mitral and tricuspid annular parameters in different end-diastolic tricuspid annular groups

Parameters	TAD-D ≤2.02 cm (n=34)	2.02 cm < TAD-D <2.66 cm (n=100)	2.66 cm ≤ TAD-D (n=25)	TAA-D ≤5.73 cm^2 (n=25)	5.73 cm^2 < TAA-D <9.03 cm^2 (n=109)	9.03 cm^2 ≤ TAA-D (n=25)	TAP-D ≤9.32 cm (n=28)	9.32 cm < TAP-D <11.66 cm (n=99)	11.66 cm ≤ TAP-D (n=32)
MAD-S (cm)	1.46±0.31*	1.64±0.39*†	1.78±0.35*†	1.52±0.39	1.63±0.38*	1.69±0.34*	1.54±0.39	1.67±0.38*	1.57±0.35*
MAA-S (cm^2)	3.00±0.96*	3.54±1.27*†	4.09±1.12*†‡	3.20±1.12*	3.53±1.21*	3.74±1.36*	3.18±0.97*	3.64±1.26*	3.41±1.29*
MAP-S (cm)	6.72±1.03*	7.14±1.22*	7.70±0.95*†‡	6.86±1.09*	7.15±1.15*	7.37±1.32*	6.79±0.97*	7.25±1.19*	7.12±1.27*
MAD-D (cm)	2.29±0.36*	2.48±0.46*†	2.43±0.31*	2.32±0.36*	2.45±0.45*	2.46±0.36*	2.43±0.46*	2.44±0.43*	2.43±0.40
MAA-D (cm^2)	6.66±1.88*	7.45±2.15†	7.50±2.35*	6.79±1.91*	7.30±2.10	7.72±2.48*	6.88±2.14*	7.29±2.12	7.63±2.19*
MAP-D (cm)	9.77±1.46	10.34±1.40†	10.37±1.64*	9.82±1.42*	10.23±1.40*	10.58±1.69*	9.81±1.51*	10.23±1.44	10.56±1.44*
MAFAC (%)	51.9±16.8*	51.3±15.0*	42.8±14.5*†‡	50.2±18.4*	49.9±15.5*	50.5±12.9*	50.7±17.0*	48.4±15.7*	54.6±13.0*‡
MAFS (%)	35.3±14.6*	32.9±15.1*	26.3±14.0†‡	34.1±14.7*	32.2±15.7*	31.2±12.4*	35.4±15.1*	30.6±15.5*	35.0±13.1*
TAD-S (cm)	1.60±0.13	1.84±0.21†	2.23±0.33†‡	1.59±0.12	1.82±0.22†	2.25±0.31†‡	1.64±0.15	1.84±0.26†	2.06±0.34†‡
TAA-S (cm^2)	4.21±1.02	5.45±1.17†	7.10±1.63†‡	3.76±0.54	5.33±1.03†	7.54±1.39†‡	3.85±0.57	5.39±1.12†	6.96±1.55†
TAP-S (cm)	8.16±0.79	9.13±0.98†	10.10±1.09†‡	7.79±0.67	9.03±0.83†	10.49±0.94†‡	7.87±0.75	9.04±0.84†	10.19±1.03†
TAD-D (cm)	1.93±0.09	2.35±0.15†	2.86±0.20†‡	2.02±0.20	2.32±0.25†	2.72±0.29†‡	2.12±0.23	2.34±0.29	2.54±0.35
TAA-D (cm^2)	5.80±1.17	7.43±1.23†	9.35±1.41†‡	5.06±0.50	7.31±0.91†	10.02±0.99†‡	5.33±0.66	7.28±1.04	9.48±1.27
TAP-D (cm)	9.68±1.14	10.49±1.01†	11.57±0.89†‡	8.88±0.53	10.48±0.80†	12.14±0.54†‡	8.85±0.46	10.41±0.64†	12.16±0.40†‡
TAFAC (%)	27.1±10.3	26.5±10.7	27.8±17.7	25.5±9.5	27.6±13.0	25.1±9.1	27.4±10.0	26.7±12.8	26.8±11.1
TAFS (%)	17.0±6.8	21.4±9.0†	21.9±8.9†	20.3±6.7	21.3±9.3	17.2±7.3‡	21.8±7.1	20.7±9.5	18.9±7.4

Data are presented as mean ± standard deviation. *, P<0.05 *vs.* TA counterpart; †, P<0.05 *vs.* matching mean – SD TA end-diastolic dimension; ‡, P<0.05 *vs.* matching mean TA end-diastolic dimension. TAD, tricuspid annular diameter; D, end-diastolic; TAA, tricuspid annular area; TAP, tricuspid annular perimeter; MAD, mitral annular diameter; S, end-systolic; MAA, mitral annular area; MAP, mitral annular perimeter; MAFAC, mitral annular fractional area change; MAFS, mitral annular fractional shortening; TAFAC, tricuspid annular fractional area change; TAFS, tricuspid annular fractional shortening; TA, tricuspid annular; SD, standard deviation.

While the mitral valve is bicuspid, the tricuspid valve has not only an anterior and posterior, but a septal leaflet as well. Furthermore, the two valves are attached to atria with different structures. While the LA fills from the four pulmonary veins, the RA fills from the superior and inferior caval veins and the coronary sinus. In addition, the two atria are emptied towards the ventricles of a different structure, as well (18). While the LV is a bullet (or egg)-shaped heart cavity made up of muscle fibers perpendicular to each other, capable of twisting and contracting (18-20), RV located around the LV on the right side of the heart, which is triangular from the sides, its cross-sectional image resembles a crescent moon, widening from the apex to the base. The RV has no rotational mechanics, its motion during the cardiac cycle reminds of a bellows (18,21-23). These fundamental differences between the right and left hearts rightly raise the possibility that the two atrioventricular annuli differ in size and function. With the present study it was examined what happens with one annulus, if the end-diastolic or end-systolic dimension and function if the other annulus is smaller or larger than the mean.

The fact that non-invasive cardiovascular imaging has developed significantly in recent decades can help us in this. Not only new methods appeared (computer tomography, magnetic resonance imaging), but significant developments were also made in echocardiography. The state-of-the-art 3DSTE is suitable not only for volumetric and strain analyses of heart cavities using spatial models, but also for 'en-face' examination of the atrioventricular valvular annuli. Although this analysis only allows 2D-projected assessment of annuli, its main advantage is its simplicity and ease of implementation (7-12).

Table 6 Mitral and tricuspid annular parameters in different end-systolic tricuspid annular groups

Parameters	TAD-S ≤1.56 cm (n=17)	1.56 cm < TAD-S <2.14 cm (n=122)	2.14 cm ≤ TAD-S (n=20)	TAA-S ≤3.93 cm^2 (n=27)	3.93 cm^2 < TAA-S <6.93 cm^2 (n=111)	6.93 cm^2 ≤ TAA-S (n=21)	TAP-S ≤7.94 cm (n=29)	7.94 cm < TAP-S <10.2 cm (n=106)	10.2 cm ≤ TAP-S (n=24)
MAD-S (cm)	1.69±0.36*	1.59±0.38*	1.76±0.38*	1.55±0.35	1.65±0.40*	1.60±0.29*	1.58±0.40	1.63±0.39*	1.64±0.33*
MAA-S (cm^2)	3.41±1.13	3.43±1.24*	4.07±1.12*‡	3.05±0.84*	3.61±1.27*†	3.58±1.31*	3.21±0.98*	3.58±1.23*	3.55±1.44*
MAP-S (cm)	7.01±1.09*	7.07±1.20*	7.66±0.98*‡	6.68±0.84*	7.22±1.20*†	7.30±1.32*†	6.78±0.96*	7.24±1.17*	7.12±1.40*
MAD-D (cm)	2.34±0.45*	2.45±0.44*	2.40±0.27*	2.36±0.43*	2.45±0.43*	2.45±0.37*	2.38±0.39*	2.46±0.44*	2.37±0.39*
MAA-D (cm^2)	6.45±1.42	7.34±2.22	7.69±2.08*†	6.41±1.72*	7.42±2.12†	7.71±2.51*†	6.78±1.93*	7.44±2.13	7.23±2.41*
MAP-D (cm)	9.59±0.97	10.25±1.50	10.56±1.51*†	9.43±1.28	10.37±1.41†	10.47±1.69*†	9.75±1.35	10.36±1.44†	10.18±1.63*
MAFAC (%)	46.7±14.2*	51.3±15.8*	45.4±14.3*	50.3±14.2*	49.5±16.6*	52.9±11.0*	50.9±13.8*	49.8±16.5*	50.3±13.5*
MAFS (%)	26.5±14.9	34.1±14.6*†	26.5±15.7*‡	33.2±14.1*	31.8±16.0*	34.1±11.1*	33.3±14.0*	32.5±15.9*	30.3±12.0*
TAD-S (cm)	1.42±0.08	1.82±0.17†	2.38±0.25†‡	1.58±0.17	1.84±0.21†	2.25±0.35†‡	1.66±0.20	1.83±0.24†	2.19±0.34†‡
TAA-S (cm^2)	3.87±0.86	5.31±1.17†	7.52±1.49†‡	3.50±0.33	5.40±0.79†	8.23±1.06†‡	3.68±0.48	5.39±0.90†	7.86±1.33†‡
TAP-S (cm)	8.18±0.88	8.99±1.00†	10.26±1.09†‡	7.63±0.59	9.09±0.71†	10.86±0.83†‡	7.47±0.38	9.10±0.55†	10.93±0.64†‡
TAD-D (cm)	2.08±0.25	2.30±0.26†	2.81±0.24†‡	2.04±0.22	2.35±0.26†	2.67±0.35†‡	2.11±0.25	2.34±0.27†	2.63±0.35†‡
TAA-D (cm^2)	5.64±1.03	7.26±1.33†	9.60±1.51†‡	5.50±0.89	7.38±1.18†	9.83±1.27†‡	5.62±1.02	7.37±1.19†	9.67±1.32†‡
TAP-D (cm)	9.35±0.74	10.45±1.07†	11.69±0.95†‡	9.16±0.73	10.53 0.94†	11.98±0.70†‡	9.22±0.79	10.51±0.92†	12.00±0.63†‡
TAFAC (%)	30.6±11.9	27.2±12.1	21.6±8.7†‡	35.1±9.7	26.0±9.5†	20.6±18.9†‡	33.4±9.7	26.1±10.1†	18.6±6.6†‡
TAFS (%)	30.5±10.4	20.1±7.9†	15.2±4.9†‡	22.3±9.2	21.1±8.7	15.5±6.4†‡	21.0±8.4	21.2±8.9	16.7±7.4‡

Data are presented as mean ± standard deviation. *, P<0.05 *vs.* TA counterpart; †, P<0.05 *vs.* matching mean – SD TA end-systolic dimension; ‡, P<0.05 *vs.* matching mean TA end-systolic dimension. TAD, tricuspid annular diameter; S, end-systolic; TAA, tricuspid annular area; TAP, tricuspid annular perimeter; MAD, mitral annular diameter; MAA, mitral annular area; MAP, mitral annular perimeter; D, end-diastolic; MAFAC, mitral annular fractional area change; MAFS, mitral annular fractional shortening; TAFAC, tricuspid annular fractional area change; TAFS, tricuspid annular fractional shortening; TA, tricuspid annular; SD, standard deviation.

The main finding of the present study is that same-side end-diastolic annular dilation is associated with simultaneous end-systolic dilation and vice versa. MA dilation in end-diastole and end-systole result in MA functional improvement/deterioration. Dilation of end-diastolic TA dimensions does not obviously entail functional differences in TA function. However, similar to MA, more dilated TA in end-systole impairs TA function. More interesting what happens with the contralateral annulus. Dilation of MA/TA dimensions does not obviously mean that contralateral TA/MA dimensions are also dilated and functionally improved/impaired. Only some parameters showed dilation tendencies and changes in function. First of all, these results suggest, that just because one annulus is more dilated, the contralateral is not in healthy subjects without regurgitation. Secondly, MA and TA behave differently: while end-diastolic and end-systolic MA dimensions expand to different degrees, leading to differences in MA function, in the case of the tricuspid valve in end-diastole, this does not happen, so the function does not change with dilation substantially. If end-systolic TA dimensions are dilated, the situation is similar.

These findings are more interesting if we analyse these data in the context of atrial volumes and function. Strong associations in case of dilation of TA/MA in the presence of higher RA/LA volumes could be demonstrated even under healthy circumstances (24,25). Pre-systolic contraction of MA is known to be associated with LA contraction and minimal MA area during early LV systole (26). Moreover, associations between RA strains in radial direction and end-diastolic TA area could be detected as well (27). Similar strong associations between MA with ventricular function

Table 7 Intra- and interobserver variability for three-dimensional speckle-tracking echocardiography-derived tricuspid annular dimensions and right atrial volumes

Parameters	Intraobserver agreement		Interobserver agreement	
	Mean ± 2SD difference in values obtained by 2 measurements of the same observer	ICC between measurements of the same observer (P)	Mean ± 2SD difference in values obtained by 2 observers	ICC between independent measurements of 2 observers (P)
MAD-D	0.03±0.18 cm	0.94 (<0.0001)	0.04±0.20 cm	0.97 (<0.0001)
MAA-D	–0.03±0.87 cm^2	0.97 (<0.0001)	0.03±0.61 cm^2	0.96 (<0.0001)
MAP-D	–0.03±0.84 cm	0.97 (<0.0001)	–0.09±0.71 cm	0.97 (<0.0001)
MAD-S	–0.03±0.11 cm	0.96 (<0.0001)	0.03±0.13 cm	0.98 (<0.0001)
MAA-S	–0.03±0.23 cm^2	0.96 (<0.0001)	–0.05±0.55 cm^2	0.96 (<0.0001)
MAP-S	0.06± 0.75 cm	0.97 (<0.0001)	0.05±0.54 cm	0.97 (<0.0001)
TAD-D	0.03±0.17 cm	0.97 (<0.0001)	0.03±0.24 cm	0.97 (<0.0001)
TAA-D	–0.03±1.11 cm^2	0.96 (<0.0001)	0.03±0.71 cm^2	0.96 (<0.0001)
TAP-D	–0.03±0.65 cm	0.95 (<0.0001)	–0.10±0.70 cm	0.97 (<0.0001)
TAD-S	–0.03±0.28 cm	0.95 (<0.0001)	0.02±0.56 cm	0.96 (<0.0001)
TAA-S	–0.03±0.40 cm^2	0.97 (<0.0001)	–0.05±0.75 cm^2	0.96 (<0.0001)
TAP-S	0.08±0.51 cm	0.97 (<0.0001)	0.05±0.41 cm	0.96 (<0.0001)

SD, standard deviation; ICC, interclass correlation coefficient; MAD, mitral annular diameter; MAA, mitral annular area; MAP, mitral annular perimeter; TAD, tricuspid annular diameter; TAA, tricuspid annular area; TAP, tricuspid annular perimeter; D, end-diastolic; S, end-systolic.

are known as well, in systole, contraction of the MA is due to shortening of the helical LV basal fibers (13,26,28). These results confirm morphological and functional connection between atria/ventricles and atriventricular annuli.

In a recent Chinese population-based study, similar prevalence of FMR and FTR were found (29). Results of the present study suggest different pattern of changes in morphology and function of contralateral atrioventricular valves if a valvular annulus is dilated. Compared to MA, more dilated TA and absence of improved TA function in response to dilation of TA in end-diastole found in the same healthy subjects could partly explain early development of FTR. However, results should be repeated in patients with FMR and/or FTR being in different degrees to see the same parameters. Findings of the present study add further insights into understanding the (patho)physiology of the development of FMR/FTR.

Although reproducibility of the presented 3DSTE-derived MA/TA analysis seems to be excellent, feasibility proved to be only 64%. This fact makes the whole analysis limited in real-life settings at this moment using Artida equipment. The main advantage of the present method is its simplicity and easy-to-perform nature, and the fact that can be performed together with chamber quantifications. That means, that in case of volumetric and functional characterization of a heart chamber, measurement of MA/TA dimensions does not require the acquisition of additional datasets, which would overcomplicate the investigation and prolong its time. The other advantage is that normal reference values for 3DSTE-derived MA/TA dimensions are also available (11,12). However, further validations against other images techniques are necessary to confirm presented findings in healthy subjects.

Limitation section

The following limitations have arisen during the investigations:

- ❖ 3DSTE-derived image quality is still worse compared to that of 2D echocardiography, which could limit its clinical usefulness. However, reproducibility of 3DSTE-derived MA/TA determination proved to be excellent (7-12).
- ❖ It was not purposed to compare 2D echocardiography and 3DSTE in determination of MA/TA dimensions either.
- ❖ Quantification of volumes or assessment of any

strains or rotational parameters of any chambers by 3D (speckle-tracking) echocardiography were not purposed in the present study (7-12).

- Both MA and TA have a spatial 3D saddle-shape, which was not taken into account, since for technical reasons only the 2D-projected image of the annuli was examined (13,15,30).
- FMR and FTR were excluded by only a visual assessment, more advanced methods were not applied during quantifications (31-33).
- Speckle-tracking-based spatial analysis of MA/TA functionality was not purposed either (34).
- Sex differences in MA/TA parameters were not examined due to limited number of subjects. Moreover, the shape of annuli was also not assessed (35).
- Although there is an important role exerted by the antero-posterior thoracic diameter in determining a different size of MA and TA, these relationships were not examined in the present study (36).

Conclusions

Dilation of MA and TA is associated with different contralateral response in morphology and function.

Acknowledgments

Funding: None.

Footnote

Reporting Checklist: The authors have completed the STROBE reporting checklist. Available at https://qims.amegroups.com/article/view/10.21037/qims-24-630/rc

Conflicts of Interest: All authors have completed the ICMJE uniform disclosure form (available at https://qims.amegroups.com/article/view/10.21037/qims-24-630/coif). A.N. serves as an unpaid editorial board member of *Quantitative Imaging in Medicine and Surgery*. The other authors have no conflicts of interest to declare.

Ethical Statement: The authors are accountable for all aspects of the work in ensuring that questions related to the accuracy or integrity of any part of the work are appropriately investigated and resolved. The study was conducted in accordance with the Declaration of Helsinki (as revised in 2013). The study was approved by the Institutional and Regional Human Biomedical Research Committee of University of Szeged (Hungary) (No. 71/2011) and informed consent was taken from all subjects.

References

1. Coisne A, Lancellotti P, Habib G, Garbi M, Dahl JS, Barbanti M, Vannan MA, Vassiliou VS, Dudek D, Chioncel O, Waltenberger JL, Johnson VL, De Paulis R, Citro R, Pibarot P; EuroValve Consortium. ACC/AHA and ESC/EACTS Guidelines for the Management of Valvular Heart Diseases: JACC Guideline Comparison. J Am Coll Cardiol 2023;82:721-34.
2. Zern EK, Frank RC, Yucel E. Valvular Heart Disease in the Cardiac Intensive Care Unit. Crit Care Clin 2024;40:105-20.
3. Sapna F, Raveena F, Chandio M, Bai K, Sayyar M, Varrassi G, Khatri M, Kumar S, Mohamad T. Advancements in Heart Failure Management: A Comprehensive Narrative Review of Emerging Therapies. Cureus 2023;15:e46486.
4. Kamde SP, Anjankar A. Pathogenesis, Diagnosis, Antimicrobial Therapy, and Management of Infective Endocarditis, and Its Complications. Cureus 2022;14:e29182.
5. Saef JM, Ghobrial J. Valvular heart disease in congenital heart disease: a narrative review. Cardiovasc Diagn Ther 2021;11:818-39.
6. Howard C, Jullian L, Joshi M, Noshirwani A, Bashir M, Harky A. TAVI and the future of aortic valve replacement. J Card Surg 2019;34:1577-90.
7. Ammar KA, Paterick TE, Khandheria BK, Jan MF, Kramer C, Umland MM, Tercius AJ, Baratta L, Tajik AJ. Myocardial mechanics: understanding and applying three-dimensional speckle tracking echocardiography in clinical practice. Echocardiography 2012;29:861-72.
8. Urbano-Moral JA, Patel AR, Maron MS, Arias-Godinez JA, Pandian NG. Three-dimensional speckle-tracking echocardiography: methodological aspects and clinical

potential. Echocardiography 2012;29:997-1010.
9. Muraru D, Niero A, Rodriguez-Zanella H, Cherata D, Badano L. Three-dimensional speckle-tracking echocardiography: benefits and limitations of integrating myocardial mechanics with three-dimensional imaging. Cardiovasc Diagn Ther 2018;8:101-17.
10. Gao L, Lin Y, Ji M, Wu W, Li H, Qian M, Zhang L, Xie M, Li Y. Clinical Utility of Three-Dimensional Speckle-Tracking Echocardiography in Heart Failure. J Clin Med 2022;11:6307.
11. Nemes A, Kormányos Á, Domsik P, Kalapos A, Gyenes N, Lengyel C. Normal reference values of three-dimensional speckle-tracking echocardiography-derived mitral annular dimensions and functional properties in healthy adults: Insights from the MAGYAR-Healthy Study. J Clin Ultrasound 2021;49:234-9.
12. Nemes A, Kormányos Á, Rácz G, Ruzsa Z, Ambrus N, Lengyel C. Normal reference values of tricuspid annular dimensions and functional properties in healthy adults using three-dimensional speckle-tracking echocardiography (insights from the MAGYAR-Healthy Study). Quant Imaging Med Surg 2023;13:121-32.
13. Silbiger JJ. Anatomy, mechanics, and pathophysiology of the mitral annulus. Am Heart J 2012;164:163-76.
14. Silbiger JJ, Bazaz R. The anatomic substrate of mitral annular contraction. Int J Cardiol 2020;306:158-61.
15. Putthapiban P, Amini MR, Abudayyeh I. Anatomy of the Tricuspid Valve and Pathophysiology of Tricuspid Regurgitation. Interv Cardiol Clin 2022;11:1-9.
16. Yucel E, Bertrand PB, Churchill JL, Namasivayam M. The tricuspid valve in review: anatomy, pathophysiology and echocardiographic assessment with focus on functional tricuspid regurgitation. J Thorac Dis 2020;12:2945-54.
17. Lang RM, Badano LP, Mor-Avi V, Afilalo J, Armstrong A, Ernande L, Flachskampf FA, Foster E, Goldstein SA, Kuznetsova T, Lancellotti P, Muraru D, Picard MH, Rietzschel ER, Rudski L, Spencer KT, Tsang W, Voigt JU. Recommendations for cardiac chamber quantification by echocardiography in adults: an update from the American Society of Echocardiography and the European Association of Cardiovascular Imaging. Eur Heart J Cardiovasc Imaging 2015;16:233-70.
18. Feigenbaum H. Echocardiography. 5th ed. Lea & Febiger, Philadelphia, 1994.
19. Stöhr EJ, Shave RE, Baggish AL, Weiner RB. Left ventricular twist mechanics in the context of normal physiology and cardiovascular disease: a review of studies using speckle tracking echocardiography. Am J Physiol Heart Circ Physiol 2016;311:H633-44.
20. Sengupta PP, Tajik AJ, Chandrasekaran K, Khandheria BK. Twist mechanics of the left ventricle: principles and application. JACC Cardiovasc Imaging 2008;1:366-76.
21. Haddad F, Hunt SA, Rosenthal DN, Murphy DJ. Right ventricular function in cardiovascular disease, part I: Anatomy, physiology, aging, and functional assessment of the right ventricle. Circulation 2008;117:1436-48.
22. Ho SY, Nihoyannopoulos P. Anatomy, echocardiography, and normal right ventricular dimensions. Heart 2006;92 Suppl 1:i2-13.
23. Foale R, Nihoyannopoulos P, McKenna W, Kleinebenne A, Nadazdin A, Rowland E, Smith G. Echocardiographic measurement of the normal adult right ventricle. Br Heart J 1986;56:33-44.
24. Nemes A, Kormányos Á, Rácz G, Ruzsa Z, Achim A, Ambrus N, Lengyel C. Tricuspid annular and right atrial volume changes are associated in healthy adults-insights from the three-dimensional speckle-tracking echocardiographic MAGYAR-Healthy Study. Front Cardiovasc Med 2023;10:1140599.
25. Nemes A, Kormányos Á, Ambrus N, Lengyel C. Associations between Mitral Annular and Left Atrial Volume Changes in Healthy Adults-Detailed Analysis from the Three-Dimensional Speckle-Tracking Echocardiographic MAGYAR-Healthy Study. Rev Cardiovasc Med 2022;23:194.
26. Mihaila S, Muraru D, Miglioranza MH, Piasentini E, Peluso D, Cucchini U, Iliceto S, Vinereanu D, Badano LP. Normal mitral annulus dynamics and its relationships with left ventricular and left atrial function. Int J Cardiovasc Imaging 2015;31:279-90.
27. Nemes A, Kormányos Á, Ruzsa Z, Achim A, Ambrus N, Lengyel C. Three-Dimensional Speckle-Tracking Echocardiography-Derived Tricuspid Annular Dimensions and Right Atrial Strains in Healthy Adults-Is There a Relationship? (Insights from the MAGYAR-Healthy Study). J Clin Med 2023;12:4240.
28. Ormiston JA, Shah PM, Tei C, Wong M. Size and motion of the mitral valve annulus in man. I. A two-dimensional echocardiographic method and findings in normal subjects. Circulation 1981;64:113-20.
29. Li W, Xiong S, Yin S, Deng W, Zhao Y, Li Z, Yang H, Zhou Y, Yu S, Guo X, Sun Y. Prevalence and Risk Factors of Mitral, Tricuspid, and Aortic Regurgitation: A Population-Based Study from Rural Northeast China. Am J Cardiol 2023;209:156-62.
30. Wang Y, Zhu Z, Niu L, Liu B, Lin J, Lu M, Xiong C,

Wang J, Cai Y, Wang H, Wu W. Geometric remodeling of tricuspid valve in pulmonary hypertension and its correlation with pulmonary hypertension severity: a prospectively case-control study using four-dimensional automatic tricuspid valve quantification technology. Quant Imaging Med Surg 2024;14:1699-715.
31. Wu Y, Meng F, Liu Y, Zuo W, Li Q, Chen B, Kong D, Wang Y, Chen H, Pan C, Dong L, Shu X. Echocardiographic parameters recommended for assessing the severity of tricuspid regurgitation: concordance and discordance. Quant Imaging Med Surg 2023;13:5089-99.
32. Toader DM. Echocardiographic quantification of mitral apparatus morphology and dynamics in patients with dilated cardiomyopathy. J Int Med Res 2024;52:3000605231209830.
33. Rudski LG, Lai WW, Afilalo J, Hua L, Handschumacher MD, Chandrasekaran K, Solomon SD, Louie EK, Schiller NB. Guidelines for the echocardiographic assessment of the right heart in adults: a report from the American Society of Echocardiography endorsed by the European Association of Echocardiography, a registered branch of the European Society of Cardiology, and the Canadian Society of Echocardiography. J Am Soc Echocardiogr 2010;23:685-713; quiz 786-8.
34. Wang Z, Hu Y, Ou H, Feng J, Dong S, Ren S, Lu G, Li J. Speckle tracking tissue motion mitral annulus displacement to assess early changes in the left ventricle and its association with lung function in patients with chronic obstructive pulmonary disease. J Clin Ultrasound 2023;51:1439-48.
35. Amin S, Dewey H, Lasso A, Sabin P, Han Y, Vicory J, Paniagua B, Herz C, Nam H, Cianciulli A, Flynn M, Laurence DW, Harrild D, Fichtinger G, Cohen MS, Jolley MA. Euclidean and Shape-Based Analysis of the Dynamic Mitral Annulus in Children using a Novel Open-Source Framework. J Am Soc Echocardiogr 2024;37:259-67.
36. Sonaglioni A, Nicolosi GL, Lombardo M, Gensini GF, Ambrosio G. Influence of chest conformation on myocardial strain parameters in healthy subjects with mitral valve prolapse. Int J Cardiovasc Imaging 2021;37:1009-22.

Cite this article as: Nemes A, Kormányos Á, Lengyel C. Comparison of dimensions and functional features of mitral and tricuspid annuli in the same healthy adults: insights from the three-dimensional speckle-tracking echocardiographic MAGYAR-Healthy Study. Quant Imaging Med Surg 2024;14(9):6780-6791. doi: 10.21037/qims-24-630

